Fracture Toughness of Powder Forged Iron-based Alloys

鐵基合金粉末鍛造鋼破裂韌性

Feng, H. P., Liao, K.-C., and Cheng, C. D.

馮慧平 廖國基 鄭春德

摘要

本研究檢視燒結鐵基合金經鍛造製程後之破裂韌性，實驗結果顯示傳統燒結合金（密度 6.44~6.78 g/cm^3）之破裂韌性約 13.1~18.2 $MPa\sqrt{m}$ ，經鍛造後（密度 7.27~7.37 g/cm^3）之破裂韌性顯著提升為 24.4~28.9 $MPa\sqrt{m}$ ，合金之密度或孔隙率可能是影響破裂韌性的主控因素。實驗亦顯示由密度為 6.44 g/cm^3 之燒結試片進行後續鍛造製程，破裂韌性具有較大之提升，其原因可能在於此試片於鍛造製程中，承受較高程度之變形所致。

關鍵詞：破裂韌性、粉末鍛造、燒結鐵基合金

ABSTRACT

Fracture toughness of sintered iron-based alloys under the forging procedure is investigated in the current study. Experiments show that the fracture toughness K_{IC} of conventional sintered iron-based alloys range from 13.1 to 18.2 $MPa\sqrt{m}$ with the associated density of 6.44 to 6.78 g/cm^3. Powder forged iron-based alloys nevertheless display significantly larger fracture toughness of 24.4 to 28.9 $MPa\sqrt{m}$ with the increasing density of 7.27 to 7.37 g/cm^3. The density or porosity possibly dominates the fracture toughness of the alloy. That the sintered specimen with density of 6.44 g/cm^3 under the forging process has a large increase in fracture toughness might be due to high degree of deformation or flow in this subsequent procedure.

Keywords：fracture toughness, powder forging, sintered iron-based alloys

1. Introduction

Manufacturing of mechanical parts via a powder metallurgy technology has advantages of high precision, high efficiency, and less cost. The process is therefore widely applied into various fields. However, residual porosity generally exhibits in the sintered alloy. These voids are regarded as defects detrimental to the corresponding mechanical properties such as strength and toughness [1~11]. Powder metallurgy with following forging was then proposed to improve the weakness described above. The further process is anticipated to reduce the void volume fraction and hence to elevate the mechanical properties of the sintered alloy. Numerous studies related to the typical mechanical properties and processing conditions of powder-forged iron-based alloys were reported in the past [12]. Based on the authors' understanding, the fracture toughness of such alloys has not been systematically presented yet. The fracture toughness of powder-forged alloys with Fe-Ni-Cu-Mo powder, commonly used in the powder metallurgy industry, is then examined here.

2. Experimental Procedures

Powders of Fe - 1.75w/oNi - 1.5w/oCu - 0.5w/oMo were mixed with 0.7w/o of zinc stearate and 0.5w/o

Feng, H. P. Mechanical Engineering Department, Mingchi University of Technology
Cheng, C. D. Mechanical Engineering Department, Mingchi University of Technology
Liao, K.-C Mechanical Engineering Department, National Yunlin University of Science and Technology

graphite in a mixer. Green compacts were then pressed uniaxially with a floating die body. The compacts were sintered in a dissociated ammonia atmosphere at 1100°C. Three compacts with different densities, 6.44, 6.55, and 6.78 *g*/cm^3, were obtained and respectively designated as the material A, B, and C hereafter. The CT-type specimens shown in Figure 1 for the fracture toughness testing and rectangular specimens with dimensions of $10\times15\times55mm$ (un-notched standard specimen according to ASTM A327M) for the impact testing based on three materials were then shaped. Figure 1 shows detailed dimensions of the CT-type specimen as well. The above compacts were subsequently processed under a close-die forging. Another three densities, 7.34, 7.27, and 7.37 g/cm^3 (with respect to the material A, B and C) were obtained and respectively designated as the material AF, BF, and CF hereafter. The CT-type and rectangular specimens based on the powder-forged alloy were also prepared.

Ultimate strength, impact energy, and hardness of both sintered and powder-forged alloys were evaluated in the experiments. Ultimate strength was measured using an Instron tensile testing machine, while impact energy was obtained via a Charpy impact testing machine under the room temperature. Hardness was probed at seven different locations on the specimen utilizing a Brinell hardness tester. Maximum and minimum values were excluded while the remaining five values were averaged as a hardness value. Each testing was conducted three times for all six materials, and mean values were calculated as listed in Table 1.

The fracture toughness assessment was carried out based on the specification ASTM-E399. The pre-cracked C-type specimen was eventually ruptured under an Instron universal testing machine, and conditional fracture toughness K_Q was then estimated. According to ASTM-E399, this value of K_Q should further equal K_{IC} under the plane strain conditions due to the width of the CT-type specimen being 15 *mm*. Microstructural characterization of the ruptured specimen was then performed on a scanning electron microscope (SEM). Moreover, an optical microscope was employed to determine the crystallographic phases of the polished specimen.

3. Results and Discussions

3.1 Sintered Alloys

Figures 2 and 3 display the microstructure of the material A and B, respectively. All figures show that ferritic and pearlitic phases are formed in the corresponding matrix. Differences of void numbers among these three materials (A, B, and C) are not so evident. However, void shapes of the material C with high density approach circle as shown in Figure 3. Table 1 shows that ultimate strength, hardness, and the fracture toughness of these materials rise along with the increasing density (decreasing porosity) as expected. On the other hand, impact energy based on these three materials is not sensitive to the density within this specified range (6.44 - 6.78 *g*/cm^3).

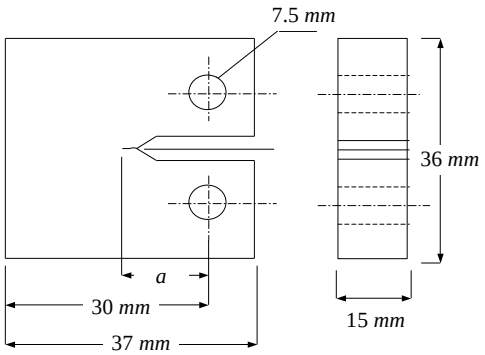

Figure 1 Dimensions of the CT-type specimen

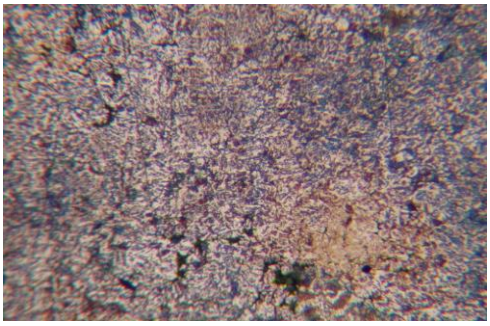

Figure 2 Microstructure of the material A (×50)

Table 1 Mechanical properties of sintered and powder-forged alloys

Material	Density (g/cm^3)	K_{IC} ($MPa\sqrt{m}$)	Ultimate Strength (MPa)	impact energy absorbed per unit area (J/cm^2)	Hardness (HB)
A	6.44	13.1	263	47.8	104
AF	7.34	24.4	705	46.2	292
B	6.55	15.9	277	46.7	114
BF	7.27	27.1	557	47.4	253
C	6.78	18.2	332	46.4	127
CF	7.37	28.9	532	48.1	229

Figures 4 to 6 show the ruptured surface of the material A, B, and C, respectively. All three figures demonstrate dimple structures representing typical ductile fracture.

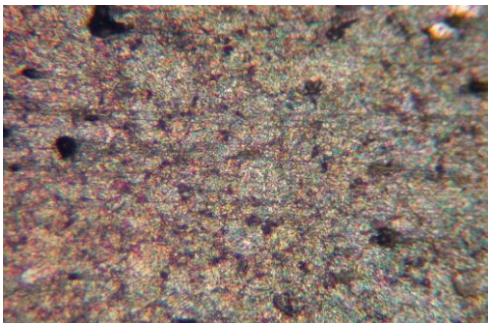

Figure 3 Microstructure of the material C (×50)

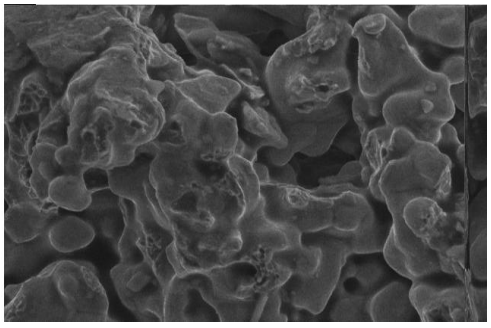

Figure 4 Ruptured surface of the material A (×2000)

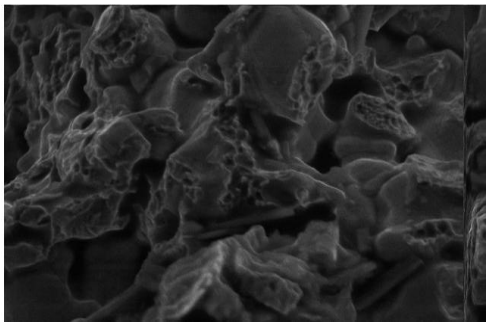

Figure 5 Ruptured surface of the material B (×2000)

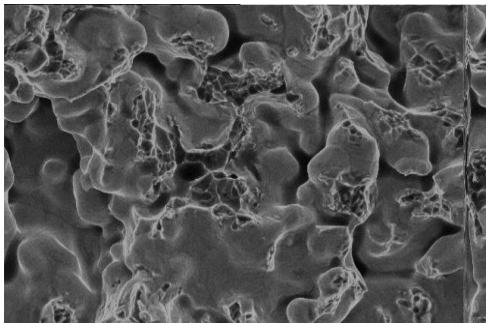

Figure 6 Ruptured surface of the material C (×2000)

3.2 Powder-forged alloys

Figures 7 and 8 display the microstructure of the material AF (7.34 g/cm^3), and CF (7.37 g/cm^3) respectively. The matrix also principally consists of ferritic and pearlitic phases as shown in the figures. Fewer voids and finer grain sizes in the

powder-forged alloys are viewed comparing to those in the associated sintered alloys. Ultimate strength, hardness, and the fracture toughness of these materials are functions of the density similar to those of the sintered alloys. Nevertheless, as listed in Table 1, the material AF has the highest ultimate strength and hardness even though it does not have the largest density. A possible reason for causing such phenomenon is that the material AF has the maximum material flow under the forging process as the corresponding density is changed from 6.44 g/cm^3 to 7.34 g/cm^3. The powder-forged alloys have about 1.5 times higher fracture toughness than the sintered ones. That the density or porosity dominates the fracture toughness could then be concluded. Impact energy based on the material AF, BF, and CF is also insensitive to the density and almost the same as that based on the material A, B, and C.

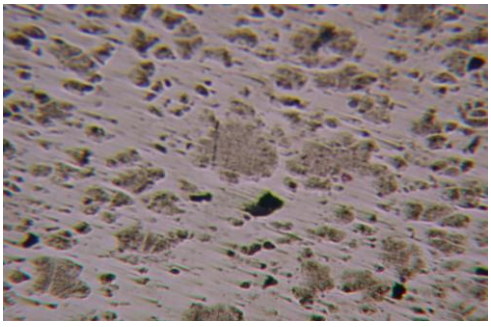

Figure 7 Microstructure of the material AF (×100)

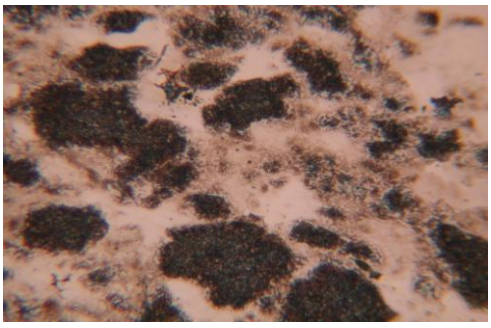

Figure 8 Microstructure of the material CF (×100)

Figures 9 to 11 show respectively the ruptured surface of the material AF, BF, and CF, and dimple structures can be also observed in these figures.

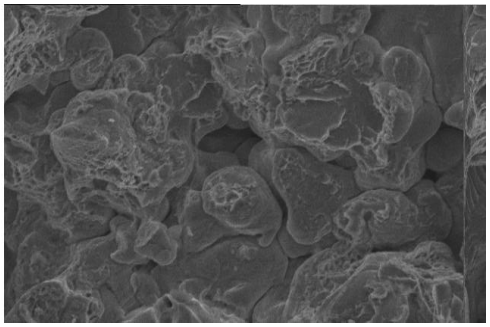

Figure 9 Ruptured surface of the material AF (×1500)

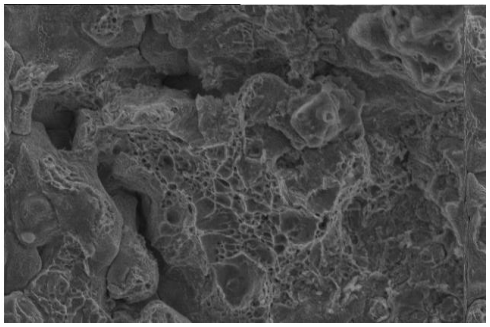

Figure 10 Ruptured surface of the material BF (×1500)

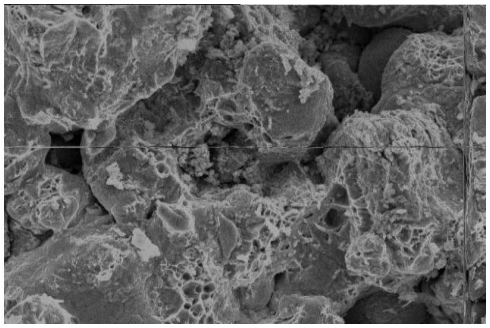

Figure 11 Ruptured surface of the material CF (×1500)

4. Conclusions

- Crystallographic phases of ferritic and pearlitic are presented in both sintered and powder forged iron-based alloys.
- Ultimate strength, hardness, and the fracture toughness of the sintered alloys rise along with the density.
- The sintered specimen with density of 6.44

g/cm^3 under the subsequent forging procedure has a large increase in fracture toughness.

- Ultimate strength, hardness, and the fracture toughness based on the powder-forging are dramatically larger than those based on the sintering. Moreover, ultimate strength seems to be strongly dependent upon the material flow as explained in the article.
- Impact energy value is not sensitive to the density within the prescribed range from 6.44 to 7.37 *g*/cm^3.

Acknowledgements

The support of this work by National Science Council of Taiwan under Grant NSC 90-2216-E-131-001- is highly appreciated.

References

1. Kuhn,H.A., Powder Metallurgy Processing Academic Press, Inc., New York., (1978)
2. Shima, S. and M.Oyane, Int. J. Mechanical Science, Vol. 18, pp.285-291, (1976)
3. Oh, H.K., J. Mech. Work. Tech., Vol. 9, pp.193-200, (1984)
4. Oh, H.K. and J. H.Mun, J. Mech.Work. Tech., Vol. 9, pp.279-290, (1984)
5. Shima, S. and M. Yamada, Powder Metallurgy, Vol. 72, pp.39-444, (1984)
6. P. Venugopal, S. Vankatraman, R. Vasudenvan and K.A.Padmanabhan, J. of Mechanical Working Technology, Vol. 15, pp.357-374, (1987)
7. M. C. Wang, Powder Metallurgy, Vol. 37, pp.201-205, (1994)
8. G. Straffelini, V. Fontanari, A. Molinari, , Powder Metallurgy, Vol. 38, pp.45-51, (1995)
9. G. Straffelini, V. Fontanari, A. Molinari, and B. Tesi, Powder Metallurgy, Vol. 36, pp.135-141, (1993)
10. F. J. Esper and C. M. Sonsino, England, EPMA, (1994)
11. R. Abdel-Karim, I. Elmanhallawi and K. El-Menshawy, Powder Metallurgy, Vol. 47, pp.43-48, (2004)
12. J. D. Bolton and M. Youseffi, Powder Metallurgy, Vol. 36, pp.142-152, (1993)